Environmental Technology & Innovation 40 (2025) 104585

Contents lists available at ScienceDirect

Environmental Technology & Innovation

journal homepage: www.elsevier.com/locate/eti

Stimulating volatile fatty acid production in anaerobic digestion: Bacterial community shifts induced by nano-zero valent iron and magnetite nanoparticles

Nicolás Hoffmann [a,b], Gustavo Ciudad [b], Paola Fincheira [b,c], Rodrigo Rodriguez [d], Christian Vergara [b], Gonzalo Tortella [b,c], Paola Durán [d,e], Cátia Sofia Neves Braga [f,g], Gilberto Martins [f,g], Lina Uribe [a,h], Olga Rubilar [b,c,*]

[a] Water Research Center for Agriculture and Mining – CRHIAM, ANID FONDAP Center, Victoria, Concepción 1295, Chile
[b] Departamento de Ingeniería Química, Universidad de La Frontera, Temuco, Chile
[c] Centro de Excelencia en Investigación Biotecnológica Aplicada al Medio Ambiente (CIBAMA), Universidad de La Frontera, Temuco, Chile
[d] Microbiología y Biocontrol de Enfermedades en Plantas, Laboratorio de Investigación en Biocontrol, Chile
[e] Departamento de Producción Agropecuaria, Facultad de Ciencias Agropecuarias y Medio Ambiente, Universidad de La Frontera, Temuco, Chile
[f] CEB - Centre of Biological Engineering, University of Minho, Braga 4710-057, Portugal
[g] LABBELS – Associate Laboratory, Braga/Guimarães, Portugal
[h] Departamento de Ingeniería de Minas, Universidad de Talca, Curicó, Chile

ARTICLE INFO

Keywords:
Iron nanoparticles
Anaerobic digestion
Volatile fatty acid
Microbial communities

ABSTRACT

The production of volatile fatty acids (VFA) through anaerobic digestion has gained significant attention due to its potential benefits for renewable energy, biofuel production, waste valorization, bioproduct synthesis, and wastewater treatment. Nano-zero valent iron (nZVI) and magnetite nanoparticles (Fe_3O_4-NPs) have been identified as effective nanomaterials for enhancing methane production, although their application in stimulating VFA production remains underexplored. This study aimed to increase VFA production by adding nZVI, Fe_3O_4-NPs, and nZVI/Fe_3O_4-NPs while investigating the associated changes in bacterial communities. AD of glucose was performed using municipal wastewater sludge over 25 days, with the sludge amended with 400 mg L^{-1} of nanoparticles. Total DNA samples were collected post-digestion to analyze bacterial community shifts. Results showed a significant enhancement of VFA production by both nZVI and Fe_3O_4-NPs, with the highest output in the Fe_3O_4-NPs treatment (811.7 mg COD L^{-1}), followed by nZVI (769.9 mg COD L^{-1}) and combined nZVI/Fe_3O_4-NPs (455.7 mg COD L^{-1}). This significant enhancement highlights the potential of these nanoparticles in waste-to-energy anaerobic digestion systems. Propionic acid was predominant in nZVI, whereas acetic acid was most abundant in Fe_3O_4-NPs. Microbial community analysis revealed *Firmicutes* as the most abundant phylum across treatments, with varying effects due to nZVI and Fe_3O_4-NPs.

* Corresponding author at: Departamento de Ingeniería Química, Universidad de La Frontera, Temuco, Chile.
E-mail addresses: n.hoffmann01@ufromail.cl (N. Hoffmann), gustavo.ciudad@ufrontera.cl (G. Ciudad), paola.fincheira@ufrontera.cl (P. Fincheira), r.rodriguez09@ufromail.cl (R. Rodriguez), christian.vergara@ufrontera.cl (C. Vergara), gonzalo.tortella@ufrontera.cl (G. Tortella), paola.duran@ufrontera.cl (P. Durán), catia.braga@ceb.uminho.pt (C.S.N. Braga), gilberto.martins@ceb.uminho.pt (G. Martins), luribe@utalca.cl (L. Uribe), olga.rubilar@ufrontera.cl (O. Rubilar).

https://doi.org/10.1016/j.eti.2025.104585
Received 4 November 2024; Received in revised form 9 September 2025; Accepted 23 October 2025
Available online 25 October 2025

1. Introduction

Valorizing wastes to produce energy or chemicals can improve both the economic and environmental performance index, moving towards the target of reaching net zero greenhouse gas emissions (Pinto et al., 2023). Recently, many studies have focused on bio-energy production (e.g., biogas and biohydrogen) and valuable product generation, such as VFAs, from organic-rich substrates via anaerobic fermentation, which is a hot topic, contributing to providing critical materials and products to replace those currently produced by fossil fuels. Focusing on VFAs production, numerous studies aim to recover organic waste by converting it into valuable products, thereby reducing waste treatment costs and fostering new economic opportunities (Du et al., 2023). VFAs are short-chain fatty acids, saturated or unsaturated carboxylic acids with six or fewer carbon atoms, including formic, acetic, propionic, butyric, valeric, and caproic acids (Feng et al., 2022). For instance, acetic and propionic acids are valuable byproducts in waste-to-energy processes and biorefineries to the sustainability movement and the circular economy. VFAs are used as the raw material for creating the building blocks of various organic compounds (e.g.: alcohols, aldehydes, ketones, and esters), to enhance renewable energy and biofuels production, waste valorization, feedstock for bioproducts, and applications for wastewater treatments (Esteban-Gutierrez et al., 2018; Chen et al., 2020). Therefore, it is remarkable that, although the main synthesis route for VFAs is based on the chemical transformation of petrochemicals, their biological synthesis has gained interest due to the applications mentioned above and the urgent need to reduce dependency on non-renewable fossil fuels (Esteban-Gutierrez et al., 2018).

VFAs are produced during the hydrolysis and acidogenesis steps of the anaerobic digestion process. Typically, they are precursors of acetate and H_2 that will be converted to methane. Thus, methanogenesis must be inhibited to avoid the conversion of VFAs to methane. The inhibition or promotion of different steps in anaerobic fermentation can be influenced by different parameters, like pH, temperature, organic loading rate, inoculum source, retention time, and operating model (Valentino et al., 2021; Garcia et al., 2023). Altering one of these parameters can directly affect microbial relationships, mainly the syntrophic interactions between bacteria and methanogens that rely on interspecies electron transfer mechanisms (IET), such as interspecies hydrogen/formate transfer (IHT/IFT) and direct interspecies electron transfer (DIET) (Alam and Dhar., 2023). This occurs because anaerobic microorganisms are susceptible to environmental fluctuations, with methanogens being the most negatively affected, as they lose their activity and disrupt the syntrophic cooperation with bacteria, thereby contributing to the accumulation of VFAs during traditional anaerobic digestion treatments.

The use of conductive materials (CM) in anaerobic-engineered systems has been widely documented as a strategy to enhance the efficiency of methane production through the anaerobic digestion process, demonstrating beneficial outcomes such as increased methane production rates (Braga et al., 2024; Hoffmann et al., 2025) and notable shifts in methanogenic community composition and IET mechanisms. However, the mechanisms underlying VFAs production in the presence of CM remain poorly understood, particularly in terms of the specific microbial pathways, interactions, and environmental factors that regulate the synthesis and accumulation of these compounds. Among all CM, ferrous nanoparticles (Fe-NPs) have been the most widely reported materials used in anaerobic digestion due to their multiple benefits (Hoffmann et al., 2022). In this sense, nano-zerovalent iron (nZVI) and magnetite nanoparticles (Fe_3O_4-NPs) are the most studied ferrous materials, and two main isolated effects can be observed. First, the dissolution of nZVI in an aqueous medium result in the production of H_2, which is necessary for promoting hydrogenotrophic methanogenesis and homo-acetogenesis, thereby enhancing the ratio of methane produced through the conversion of CO_2 into CH_4 (Eljamal et al., 2024). On the other hand, Fe_3O_4-NPs could act as electron shuttles in the cell membrane of methanogens to facilitate DIET (Wang et al., 2018). Additionally, Fe_3O_4-NPs enhanced acetoclastic methanogenesis via DIET by substituting for the roles of pili and c-type cytochromes in the dry anaerobic digestion of sewage sludge (Zhou et al., 2024). This partially clarifies the reasons behind the increased methane content within the produced biogas after adding Fe-NPs. However, the potential applications of these strategies to enhance VFAs production have been minimally explored in recent years, and a deeper understanding is still required. Advancements in the anaerobic fermentation field will likely depend on further research into the underlying biological processes and optimization of operational conditions. Gaining insight into microbial interactions, metabolic pathways, and the influence of environmental factors will be crucial for fully harnessing these strategies to achieve efficient and scalable production of VFAs.

Within this context, this study focused on the production of VFAs and microbial community distribution to provide a reference for unraveling the effects of nZVI and Fe_3O_4-NPs addition on anaerobic fermentation systems. Our experiments were designed to induce varying levels of VFAs accumulation by adding nZVI and Fe_3O_4 nanoparticles. The objective was to clarify the impact of Fe-NP supplementation on the conversion of organic matter into VFAs and to evaluate the changes in bacterial community dynamics in response to this supplementation.

2. Materials and methods

2.1. Inoculum and nanomaterials

The inoculum used in the experiments was obtained from the activated sludge of the Municipal Wastewater Treatment Plant in Temuco, Chile. The volatile solids (VS) content of the sludge was 0.02 gVS g^{-1} sample. A synthetic anaerobic medium (1.52 g COD L^{-1}), prepared according to Wang et al. (2021), was used as the substrate. The composition of the culture medium was as follows (mg L^{-1}): glucose (1500), NH_4HCO_3 (360), KH_2PO_4, $NaHCO_3$ (1000), $CaCl_2$ (7.5), N_2NiO_6*$6H_2O$ (0.5), $MnCl_2$*$4H_2O$ (0.5), $FeCl_2$*$7H_2O$ (0.5), $ZnSO_4$*$7H_2O$ (0.1), H_3BO_3 (0.1), $(NH_4)Mo_7O_{24}$ (0.05), $CuSO_4$*5H2O (0.005).

The nZVI (diameter = 40–60 nm, 99 % purity) and Fe_3O_4-NPs (diameter = 30–50 nm, 99 % purity) were purchased from Merck Sigma-Aldrich Co., Ltd (USA).

2.2. Experimental setup for acidogenesis and acetogenesis stages

To evaluate the impact of iron nanomaterials on acidogenesis, 2-bromoethane sulfonate (2-BES) was introduced at a concentration of 50 mM at the start of the experiment to inhibit methanogenesis for 25 days (Wang et al., 2021). The experiment was conducted in 250 ± 5 mL serum bottles, with each bottle receiving 83 mL of working volume, and the sludge concentration was maintained at 2.5 gSV L^{-1} , with 1.5 gSV $L^{-1}$of substrate to achieve an ISR of 1.67. Three reactors without 2-BES served as blanks. Additionally, three separate anaerobic fermentation batch tests were carried out, each involving the incorporation of a single dose of nZVI, Fe_3O_4-NPs, and a combination of nZVI/Fe_3O_4-NPs (1:1 g). A control group without nanoparticle addition was also included. A total of 15 experimental units were randomly distributed across the study. The combined nZVI/Fe_3O_4-NP treatment aimed to elucidate the synergistic effects of adding iron nanoparticles to anaerobic digestion reactors. In contrast, the treatments with nZVI and Fe_3O_4-NPs seek to determine their impacts. All treatments considered 400 mg L^{-1} of previously ultrasonicated Fe-NPs for 30 s at 40 KHz. To maintain strict anaerobic conditions, a nitrogen/dioxide carbon gas mixture (80/20) was flushed into the reactor for two minutes, and then the bottles were sealed with rubber stoppers. The bottles were placed in a water bath shaker at 37°C and stirred at 150 rpm for 25 days.

The concentration of VFAs, including acetic, propionic, butyric, valeric, and iso-valeric acids, was determined using gas chromatography (GC Clarus 400) equipped with a flame ionization detector (PerkinElmer) and a capillary column (30 m x 0.25 mm×0.25 µm, Supelco). The column, injector, and detector temperatures were set to 80 °C, 250 °C, and 250 °C, respectively, with nitrogen as the carrier gas. The operational conditions were as follows: injection volume of 1 µL, oven temperature ramp from 80 °C to 110 °C at 5°C min^{-1}, then to 138 °C at 1°C min^{-1}, with a total analysis time of 34 min. VFAs quantification was performed using an external standard (Supelco VFA mix, 10 mM), including acetic, propionic, isobutyric, butyric, isovaleric, valeric, isocaproic, caproic, and heptanoic acids. Calibration curves were generated for each VFAs in the 0–5 mM range, using a 3 % formic acid solution to improve peak resolution. VFAs concentrations were calculated according to the methodology outlined by García et al. (2023): acetic acid (1.067 gCOD g^{-1}), propionic acid (1.514 gCOD g^{-1}), butyric acid (1.818 gCOD g^{-1}), and iso-valeric acid (2.039 gCOD g^{-1}). The results were validated through analysis of variance (ANOVA), with mean comparisons performed using Tukey's test ($p < 0.05$). All samples were extracted using a syringe at intervals of 4, 6, 12, and 25 days, and then were pretreated by filtration through a 0.2 µm filter before analysis. Methane production was not measured during the experiment since methanogenesis was inhibited by adding 2-BES.

2.3. Metabarcoding analysis

Metabarcoding analysis was employed to comprehensively analyze the microbial communities involved in the anaerobic fermentation process under the influence of different iron nanoparticles. This approach enabled the identification and comparison of bacterial and archaeal communities through DNA-based techniques, providing insights into how these microbial populations responded to the addition of iron nanoparticles. Total genomic DNA samples from nZVI, Fe_3O_4-NP, nZVI/Fe_3O_4-NP, and 2-BES control were obtained after 25 days of AD. The initial sludge DNA was obtained from the activated sludge used as inoculum. Samples were extracted using MO BIO PowerSoil DNA Isolation Kit (Qiagen). The DNA samples were sent to IMR (Integrated Microbiome Resource, Canada) to be amplified the target V3-V4 regions of 16S rRNA gene using B341F (5′ CCTACGGGNGGCWGCAG 3′) and B805R (5′ GACTACHVGGGTATCTAATCC 3′) to explore bacterial communities, and the region of V6V8 regions of 16S rRNA gene using A956F (5′ TYAATYGGANTCAACRCC 3′) and A1011R (5′ CRGTGWGTRCAAGGRGCA 3′) to explore archaeal communities. The resulting amplicons were sequenced in an Illumina MiSeq platform in paired-end mode for 300 cycles.

The raw reads underwent processing utilizing the USEARCH-UNOISE3 pipeline (Edgar, 2016). This pipeline involved reconstructing amplicon sequences based on their ends with a minimum overlap of 50. This was followed by removing sequences exhibiting an expected error exceeding 1 (EE = 1), dereplicating the sequences, and eliminating chimeric sequences. Subsequently, the resulting sequences were denoised by applying the UNOISE3 algorithm, generating zero-radius OTU sequences. Taxonomic classification was accomplished using a Naïve Bayes classifier trained with the SILVA 138 database (Pruesse et al., 2007). The phylogenetic relationships between the OTU were obtained by constructing a phylogenetic tree using the FastTree algorithm (Price et al., 2009) based on a masked alignment constructed with MAFFT (Katoh and Standley, 2013).

The samples were standardized through rarefaction to a sampling depth of 50.542 for Archaea and 30.873 for Bacteria. Alpha diversity metrics, including Shannon's Diversity index for diversity and Pielou's Evenness for Evenness, were computed using the QIIME2 core-metrics function (Bolyen et al., 2019). The significance of treatment differences was assessed via permutational multivariate analysis of variance PERMANOVA with 999 random permutations on the robust Aitchison dissimilarity matrix, employing the adonis function from the vegan package (Oksanen et al., 2022) and the zero-inflated Gaussian mixture model (ZIGMM) (Paulson et al., 2013). Additionally, community exploration was conducted using LEfSe (Segata et al., 2011) to identify biologically relevant features within each group, utilizing a Kruskal-Wallis test followed by a Wilcoxon rank-sum test for pairwise comparisons, with a significance threshold of 0.05 and a linear discriminant analysis score of 2.0 to determine discriminant features. ZIGMM was implemented in the metagenomeSeq R package using cumulative sum scaling (CSS) normalized abundances.

2.4. Calculation

Acidification efficiency (AE, %) was evaluated by the following Eq. (1):

$$AE(\%) = \frac{COD_{VFAs}}{COD_{Influent}} x100\% \quad (1)$$

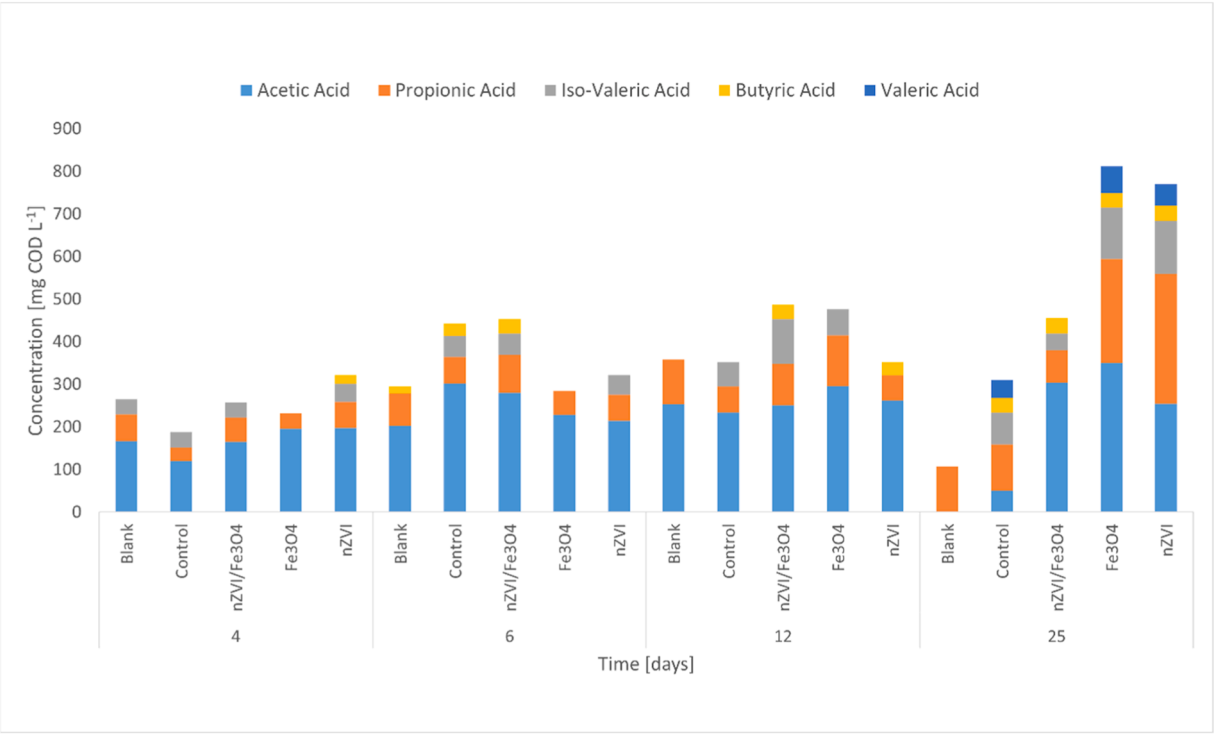

Fig. 1. VFA composition via AD reactors amended with nZVI, Fe_3O_4-NPs, nZVI/Fe_3O_4-NPs.

Where $COD_{influent}$ is the initial concentration of influent COD (mg L^{-1}), COD_{VFAs} is the concentration of effluent VFAs (mgCOD L^{-1}). Finally, all statistical analyses were performed using Prism 9.4.0 software ($p > 0.05$).

3. Results

3.1. Effect on nZVI, Fe_3O_4-NPs, and nZVI/Fe_3O_4 on VFA production

After 25 days of anaerobic incubation, the production of VFAs was mainly composed of acetic acid, propionic acid, iso-valeric acid, butyric acid, and valeric acid. Fig. 1 shows the VFAs production and composition on days 4, 6, 12, and 25. The assays with Fe_3O_4-NPs observed the highest VFAs concentration, followed by nZVI, nZVI/Fe_3O_4-NPs, control, and blank treatments, with values of 811.7, 769.9, 550.8, 455.7, and 106.9 mg COD L^{-1}, respectively. The addition of nZVI and Fe_3O_4-NPs significantly increased VFAs production compared to the control after 25 days of incubation. Additionally, the nZVI/Fe_3O_4-NPs treatment showed no significant differences compared to the control, rather than the nZVI and Fe_3O_4-NPs conditions. Based on the highest AE%, the nZVI and Fe_3O_4-NP treatments achieved conversion rates of 53.7 % and 50.9 %, respectively, with no statistically significant difference ($p > 0.05$). The combined nZVI/Fe_3O_4-NP treatment resulted in a lower % conversion rate of 30.1 %, while the control and blank assays showed conversion rates of 25.5 % and 7.1 %, respectively. As expected, adding 2-BES effectively inhibited methanogenesis, leading to the accumulation of VFAs. Moreover, all experiments involving Fe-NP supplementation demonstrated varying production levels of acetic, propionic, iso-valeric, butyric, and valeric acids. The detailed results for each experiment are provided below.

3.1.1. nZVI effect on VFA production

The nZVI treatment resulted in a total VFAs production of 769.9 mg COD L^{-1}, representing 50.9 % of the AE. By comparing the results with the control and blank conditions, the global production of VFAs was significantly increased. Specifically, propionic acid was the primary VFA produced, accounting for 306.2 mg COD L^{-1} after 25 days of incubation. Significant differences were observed in the combined treatment with nZVI/Fe_3O_4-NPs. A considerable increase in propionic acid was observed after day 12 of digestion, followed by acetic acid, which represented the second VFAs proportion at 253.7 mg COD L^{-1}. Additionally, nZVI treatment demonstrated an increased acetic acid concentration regarding control and nZVI/Fe_3O_4-NPs. In this regard, the highest iso-valeric acid production reached 124.1 mg COD L^{-1}, which was feasible to accumulate during the experiment.

Interestingly, nZVI treatment showed significant butyric acid production at the early stage of digestion ($p < 0.05$). However, at the end of the experiment, no significant differences were observed among the other treatments, suggesting that the production effect was not yet evident at this stage by adding nZVI. Finally, the addition of nZVI registered 50.4 mg COD L^{-1} of valeric acid at the end of the experiment.

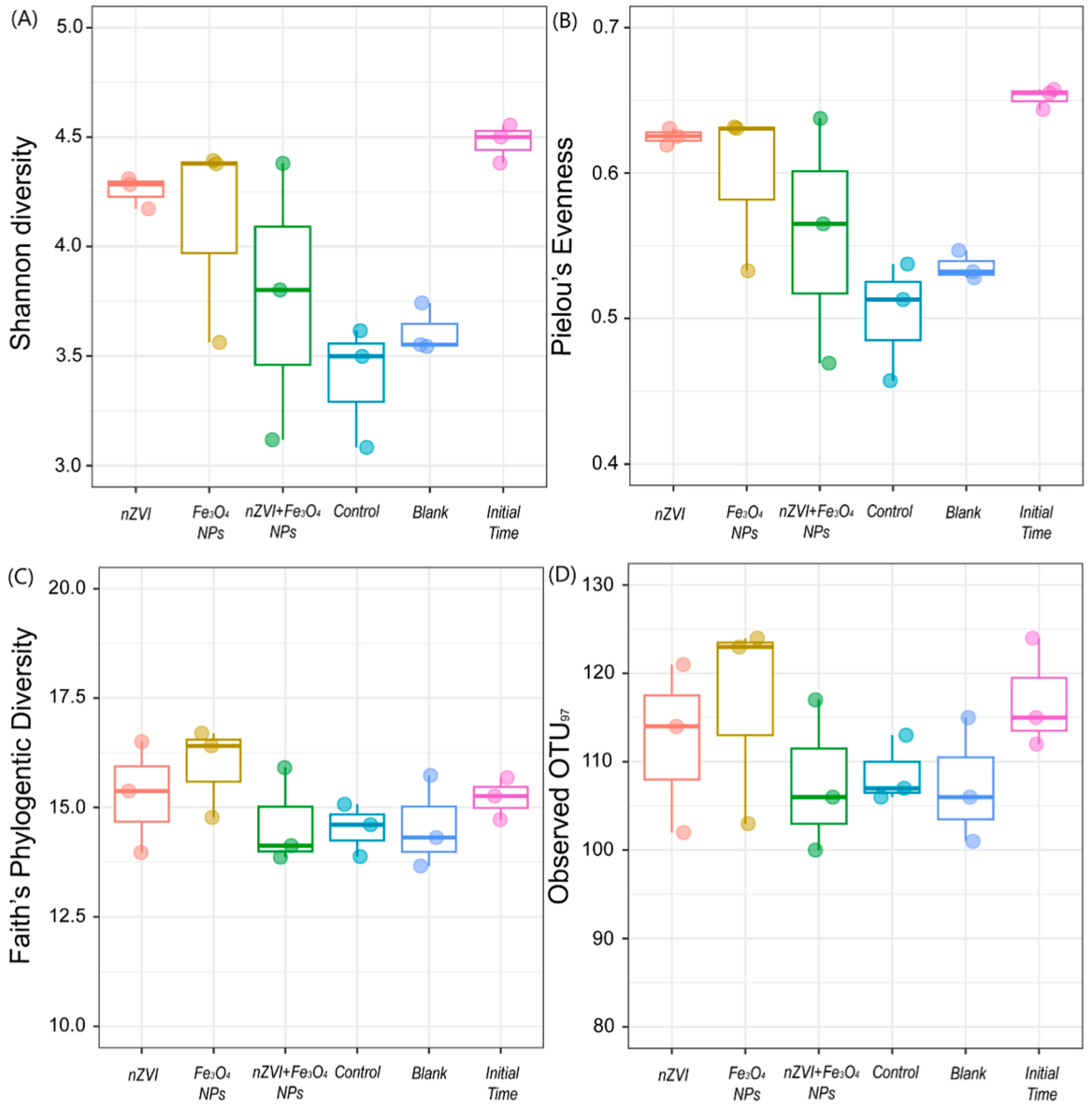

Fig. 2. Anaerobic bacterial Shannon (a), Evenness (b), Faith's (c), and OUT's (d) indexes.

3.1.2. Fe_3O_4-NPs effect on VFA production

The Fe_3O_4-NPs treatment yielded 811.7 mg COD L^{-1}, representing the highest VFAs production during anaerobic fermentation, which accounted for 53.7 % of AE conversion ($p < 0.05$). Although Fe_3O_4-NPs were demonstrated to improve the VFAs production, no significant differences were determined regarding nZVI addition. Compared to the nZVI treatment, acetic acid was the principal compound in the Fe_3O_4-NPs treatment, with a concentration of 349.8 mg COD L^{-1}, and significant differences were observed compared to the control assays. Propionic acid evidenced a concentration of 244.3 mg COD L^{-1}, demonstrating that the Fe_3O_4-NP treatment could increase the propionic acid production regarding the nZVI/Fe_3O_4-NPs ($p < 0.05$). In addition, iso-valeric and valeric output was detected. Non-significant differences were observed in iso-valeric and valeric acid production regarding the control treatment.

3.1.3. nZVI/Fe_3O_4-NPs effect on VFA production

The combined nZVI/Fe_3O_4-NPs treatment produced 455.7 mg COD L^{-1}, showing 30.1 % of VFAs production. Despite the combined treatment presenting iron as the primary compound, no significant differences were observed compared to the experimental control. Indeed, the VFAs production was lower than the remaining Fe-NPs ($p < 0.05$). Its detailed VFAs production consisted of acetic, propionic, iso-valeric, and butyric acid, with COD levels of 303.6, 76.1, 39.3, and 36.7 mg L^{-1}, respectively. Acetic acid production

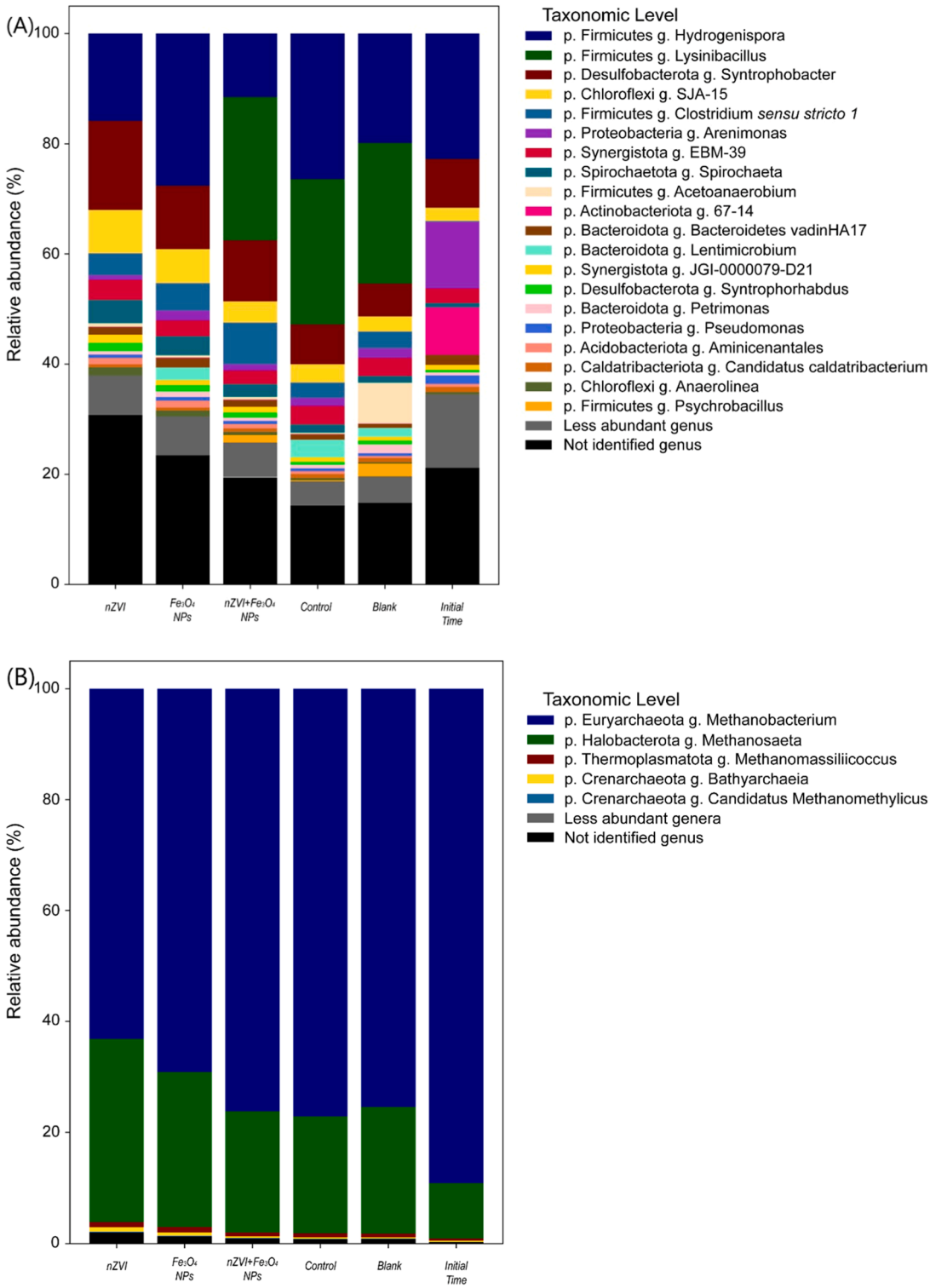

Fig. 3. Anaerobic bacterial (a) and archaeal (b) composition at the genus level.

significantly increased by adding nZVI/Fe_3O_4-NPs compared to the control assay. Butyric acid production showed no significant variation, and valeric acid production was not observed.

3.1.4. Microbial community shifts and their impact on VFA production

The metabarcoding analysis revealed significant shifts in microbial community composition in response to adding nZVI and Fe_3O_4-NPs during anaerobic fermentation (Fig. 2). In general, the Shannon index decreased as the fermentation was carried out. Initially, the inoculum showed a Shannon index of 4.48 compared to the 3.61 observed at the end of the blank assay. Alpha biodiversity was not altered by the 2-BES addition ($p > 0.05$). In the Fe-NP treatments, the Shannon index did not decrease significantly, with values of 4.25, 4.11, and 3.77 for nZVI, Fe_3O_4-NP, and nZVI/Fe_3O_4-NP, respectively. In addition, nZVI and Fe_3O_4-NP showed a higher Shannon index than nZVI/Fe_3O_4-NP ($p > 0.05$). In terms of Pielou's Evenness, the obtained values were 0.63, 0.60, and 0.56 for the nZVI, Fe_3O_4-NP, and nZVI/Fe_3O_4-NP treatments, whereas 0.50, 0.56, and 0.65 were observed for control, blank, and inoculum samples, respectively. However, rather than the significant difference observed between the control and the inoculum, the Fe-NP treatments showed no differences from the controls ($p < 0.05$). Faith's Phylogenetic Diversity values showed no significant differences between the controls and treatments, demonstrating no increase in phylogenetic tree units when applying Fe-NPs. In this context, the amount of observed OTU97 decreased significantly as the AD reaction occurred, especially noted in the blank and control assays. However, the Fe_3O_4-NP treatment showed the same OTU amount as the inoculum. In summary, (i) the Fe-NP treatments evidenced differences in the α-diversity among them and between the control measures, (ii) the Fe-NP treatment showed no differences in the microorganisms' distribution, (iii) Fe-NP treatments showed no effect on phylogenetic unit trees, and (iv) Fe_3O_4-NPs treatment showed an increase in the OTU amount during anaerobic fermentation regarding all the treatments and controls.

3.1.4.1. Bacterial communities. Furthermore, a comprehensive comparison of all treatments with the control (2-BES), blank, and initial inoculum was conducted to understand the changes in the microbial communities. This approach allowed us to observe a clear differentiation in microbial communities among nZVI, Fe_3O_4-NPs, and nZVI/Fe_3O_4-NPs addition as the anaerobic fermentation progressed (Fig. 3a). The relative abundance results of the anaerobic sludge taxa, phylum, and gender level changed according to the Fe-NP material added. Seven prominent bacterial phyla dominated all reactors of this study. The *Firmicute* phylum was relatively the most abundant taxa in all the anaerobic sludge samples (23–61 %), followed by *Desulfobacterota* (7–20 %), *Nitrospirota* (5–12 %), *Spirochaetota* (5–15 %), *Chloroflexi* (4–12 %), *Proteobacteria* (2–18 %), and *Actinobacteriota* (1–15 %). In addition to bacterial community shifts, Fig. 3b revealed that the archaeal community was primarily composed of *Euryarchaeota Methanosaeta* and *Halobacterota Methanobacterium*.

Our findings also highlighted significant changes in the initial microbial community of the inoculum. The distribution was as follows: *Firmicute Hydrogenisphora* (23 %), *Desulfubacterota Syntrophobacter* (9 %), *Proteobacteria Arenimonas* (12 %), *Actinobacteriota* 67–14 (9 %), and *Synergistota EBM-19* (3 %). The control assay was composed of *Firmicute Hydrogenisphora* (26 %), *Firmicute Lysinibacillus* (20 %), *Desulfubacterota Syntrophobacter* (7 %), *Chloroflexi SJA-15* (3 %), *Firmicutes Clostridium sensu stricto* (3 %), *Synergistota EBM-19* (3 %). Notably, a significant increase in the *Firmicute* phylum population was observed between the control and blank measures after the digestion, representing the maximum proportion among all the experiments (61 %). The inoculum exhibited differences across all treatments and controls. The amount of *Actinobacteriota, Myxococcota, and Planctomycetota* phylum significantly decreased once AD started ($p < 0.05$). Specifically, *Anaeromyxobacter, Arenimonas*, and *Leucobacter* genera significantly diminished among all the treatments. The results obtained from nZVI and Fe_3O_4-NP treatments showed similar proportions among the whole microbiome. The combined treatment (nZVI/Fe_3O_4-NP) showed no significant differences compared to the control and blank assays.

3.1.4.2. Impact of nZVI on the population dynamics of anaerobic bacterial communities. As was mentioned above, the relative abundance was dominated by *Firmicute* phylum, followed by *Desulfobacterota, Nitrospirota, Spirochaetota, Chloroflexi, Proteobacteria*, and *Actinobacteriota*, with 23 %, 20 %, 12 %, 15 %, 12 %, 2 %, and 3 %, respectively. In this regard, nZVI treatment showed significant increases in phylums *Desulfobacterota, Spricochaetota, Caldisericota*, and *Verrucomicrobiota*. Nonetheless, a significant decrease can be observed in the *Firmicute* phylum, reaching the same levels as the samples from the blank assay.

The central *Firmicutes* genders identified were *Hydrogenispora, Clostridium sensu stricto*, and *Acetoanaerobium*, with a relative abundance of 16 %, 4 %, and 0.7 %, respectively. Meanwhile, by a 16 % and 2 % phylum, *Desulfobacterota Syntrophobacter* and *Desulfobacterota Syntrophohabdus* gender were quantified as the second most considerable proportion. In addition, 8 % and 1 % of the phylum *Chloroflexi SJA-15* and *Chloroflexi Anaerolinea* genus were identified as the third significant amount. Subsequently, *Spirochaetota Sprirochaeta* genus presence reached a 4 % relative abundance, followed by 4 % and 2 % *Synergistota EBM-89* and *Synergistota JGI-0000079-D21*. The *Acidobacteriota Aminicenatales* proportion is 1.1 %. In this regard, *Chloroflexi SJA-15*, *Chloroflexi Anaerolinea*, *SJA-28*, *Desulfobacteriota Smithella propionica*, *Spirochaetota Spirochaeta*, *Desulfobacterota Syntrophobacter*, and *Desulfobacterota Syntrophorbardus* evidenced a significant increase compared to all other Fe-NP treatments and controls.

3.1.4.3. Impact of Fe_3O_4-NPs on the population dynamics of anaerobic bacterial communities. The *Firmicute* phylum dominated the microbial community, followed by *Desulfobacterota, Spirochaetota, Chloroflexi, Nitrospirota, Proteobacteria*, and *Bacteroidota*, with 35 %, 15 %, 11 %, 10 %, 9 %, respectively. The Fe_3O_4-NP treatment showed non-significant differences in phylum classification. Considering the bacterial genus classification, the *Firmicutes* phylum relative abundance was 27 % and 5 % for *Hydrogenisphora* and *Clostridium sensu stricto*, respectively. Considering the *Desulfobacterota* phylum, the genera *Syntrophobacter* and *Syntrophohabdus accounted for* 12 % and 1 %, respectively. Besides, 6 % and 1 % of the phylum *Chloroflexi SJA-15* and *Chloroflexi Anaerolinea* genus were the third

significant amount. The presence of *Spirochaetota* in the *Spirochaeta* genus reached a 3 % relative abundance, followed by *3 %* and *1 %* for *Synergistota EBM-89* and *Synergistota JGI-0000079-D21,* respectively. In this sense, *Firmicute UCG-010* increase was determined for all the other treatments ($p < 0.05$).

3.1.4.4. Impact of nZVI/Fe_3O_4-NPs on the population dynamics of anaerobic bacterial communities. By considering *Firmicutes, Desulfobacterota, Nitrospirota, Spinochaetota, Chloroflexi, Synergistota*, and *Bacteroidota* as 50 %, 13 %, 9 %, 8 %, 6 %, 3 %, and 3 %, respectively, the nZVI treatment composition results showed non-significant differences compared to the control and Fe-NPs treatments. Considering the genus classification composition, *Firmicutes Hydrogenisphora*, *Firmicutes Lysinibacillus*, and *Clostridium sensu stricto* represent 28 %, 26 %, and 5 % of the relative abundance. However, the presence of *Lysinibacillus* was detected (26 %) in the Firmicutes' gender composition, which differed from the other Fe-NP treatments. The presence of *Lysinibacillus* is also shown in control and blank samples. The *Desulfobacterota* genus phylum composition consisted of *Syntrophobacter* and *Syntrophohabdus*, representing 12 % and 1 % of the relative abundance, respectively. A 6 % and 1 % relative abundance composition was determined in *Chloroflexi SJA-15* and *Chloroflexi Anaerolinea*. In this sense, *Spirochaeta's* presence reached 3 %. The nZVI/Fe_3O_4-NP treatment showed no significant differences between the other Fe-NPs and the control measures.

4. Discussion

nZVI and Fe_3O_4-NPs are among the most effective Fe-NPs used to enhance the performance of anaerobic digestion, playing a dual role by accelerating microbial activity and promoting the conversion of organic matter. The beneficial one acts as a cofactor to promote the conversion of CO_2 into CH_4, while the adverse one promotes the generation of free radicals. This understanding can encourage the presence of specific microorganisms and inhibit others, thereby modifying the production of VFAs. It is widely accepted that nZVI and Fe_3O_4-NP supplementation affect the structure of the indigenous microbial communities (Barrena et al., 2021). In this sense, introducing Fe-NPs acts as redox mediators, facilitating the rapid conversions of VFAs, promoting the biofilm formation, which enhances microbial colonization and stability under fluctuating conditions. This innovation is particularly relevant in optimizing industrial-scale VFA production, where improving process stability can increase waste valorization and reduce greenhouse gas emissions.

4.1. Influence of Fe-NPs on VFA production

The anaerobic degradation of organic matter yields intermediate compounds consisting of VFAs and alcohols, which could be converted into H_2 or formate and finally to CH_4 and CO_2 by the syntrophic consortia. Our findings showed a similar VFAs composition reported by Du et al. (2023), generally composed of acetic acid, propionic acid, butyric acid, valeric acid, and iso-valeric acid. The findings showed a maximum of 53–54 % of AE after 25 days, and this increased when Fe-NPs were added. The exception is the combined nZVI/Fe_3O_4-NPs treatment, where a 30 % AE was obtained. Applying the combined treatment (nZVI/Fe_3O_4-NPs) showed no potential to improve VFAs production and shifts in methanogenic archaeal relative abundance, which is likely due to excessive production of reactive oxygen species that strongly affects cell membranes (Barrena et al., 2021). The proportions of propionic acid and butyric acid declined, as they can be converted to acetic acid by acetogenic species (Du et al., 2023). The Gibbs free energy of propionate oxidation, which occurs below the ATP synthesis threshold in microbial cells, is considered one of the rate-limiting steps in anaerobic fermentation. This energetically unfavorable reaction slows down the overall process, particularly affecting the production of specific VFAs. As a result, it plays a crucial role in determining the overall efficiency of anaerobic fermentation (Jin and Lu, 2023). Therefore, a syntrophic partnership must consume the remaining hydrogen and formate to a sufficiently low concentration to improve propionate oxidation. In this sense, propionic acid accumulation can completely inhibit acetic acid production, as observed in our 2-BES control assays after 25 days of incubation (Fig. 1), where the proportion of propionic acid reached twice that of acetic acid. On the contrary, nZVI and Fe_3O_4-NPs consistently accumulated propionic acid, suggesting an alteration in the microbiome structure.

4.2. Bacterial and archaeal communities' structure responses

Generally, the Shannon index tends to increase once the anaerobic fermentation begins. Therefore, the initial point significantly decreased regarding all the controls and Fe-NP treatments. Specifically, control, blank, and nZVI/Fe_3O_4-NP showed no differences. Pielou's Evenness index evidences the same behavior as the Shannon index; therefore, nZVI and Fe_3O_4-NP treatments increase the species community distribution ($p < 0.05$). The Faith's phylogenetic diversity results showed no differences between the controls and the Fe-NP treatments during the experiment. Additionally, the observed OTU classification reveals minimal differences between nZVI treatment and Fe_3O_4-NP, with values ranging from 9 to 12. Our results confirm the existence of changes in bacterial community structure due to the application of nZVI and Fe_3O_4-NP. Interestingly, the combined nZVI/Fe_3O_4-NP treatment showed no differences compared to the control and blank assays, which differs from other nanoparticle studies (Zhu et al., 2021). Regarding the improvement of VFAs production, the bacterial community responds positively to the nZVI and Fe_3O_4-NP treatments, as evidenced by increased VFAs concentration and diversification. The Shannon indices of nZVI and Fe_3O_4-NP were 4.25 and 4.11, respectively, compared to the control of 3.61, indicating a widespread microbial community that can significantly increase VFAs production. As observed, this NP can accelerate organic transformation via enriching syntrophic relationships between specific microorganism groups.

Fig. 3 shows a phylum-level analysis demonstrating that *Firmicutes* was the most dominant bacterial phylum in all the experiments and controls, accounting for 23–61 %. *Firmicutes*, the most common hydrolytic bacteria in anaerobic fermentation, are known for their

electroactive capacity and are involved in the hydrolytic and acidogenic pathways that utilize carbohydrates, proteins, and lipids to produce VFAs, CO_2, and H_2 (Kang et al., 2021). Usually, the presence of *Firmicutes* phylum increases due to the carbohydrate hydrolysis requirement. Due to the requirements for glucose fermentation and VFAs production, the *Firmicutes* population increases from 25 % to 60 % in the control. However, a significant decrease was observed in the presence of nZVI and Fe_3O_4-NP compared with the control, from 60 % to 23 % ($p < 0.05$). Similar results were observed by Barrena et al. (2021). Further, at the genus level, the relative abundances were *Hydrogenispora, Lysinibacillus*, and *Clostridium sensu stricto*. *Hydrogenispora* is associated with acetogenic production, which can ferment carbohydrates, ethanol, and H_2 to produce acetic acid. On the contrary, *Lysinbacillus* are known to degrade VFAs, alcohols, and acetate to produce H_2, which is then used by hydrogenotrophic methanogens to produce methane (Omondi et al., 2020). Therefore, as in the nZVI and Fe_3O_4-NP treatment, its absence entails increased VFAs concentration. *Clostridium sensu stricto 1* consists of strictly anaerobic, fermenting bacteria that can sporulate. These bacteria appear as straight to slightly curved rods and are significant in various habitats due to their metabolic versatility and ability to produce fermentation products, such as butanol (Wiegel et al., 2006). Their functions are related to producing H_2 from glucose degradation, and their growth and metabolism are promoted by Fe^{+3} presence (Jin et al., 2024); however, the present work showed a non-significant increase due to Fe-NPs presence.

Propionic degradation is primarily carried out by *Syntrophobacter*, a key player in syntrophic propionate oxidation, and in a process involving microbial interactions where one organism degrades organic compounds to produce substrates for another organism to utilize. Our results indicate an increase from 6 % to 7 % (control and blank assays) to 16 % when nZVI was added, suggesting that the *Synytrophobacter* growth was induced by the nZVI application, regardless of the 2-BES methanogenic inhibition, and this increase led to higher VFAs production. Species within the *Desulfobacterota* phylum engage in syntrophic relationships for propionate oxidation, a process known as syntrophic propionic-oxidizing bacteria (Kim et al., 2022). These microorganisms are typically found in anoxic conditions and can utilize sulfate, sulfite, or iron as terminal electron acceptors in respiratory processes or fermentative activities. Therefore, the anaerobic oxidation of VFAs is thermodynamically constrained. Consequently, syntrophs are characterized as growth microorganisms and classified as members of the "rare biosphere" subcommunity in natural environments (Jin and Lu, 2023). Studies have shown that syntrophic oxidizing bacteria exhibit two metabolic pathways: the methyl malonyl-CoA (MMC) pathway and C6 dismutation, with the MMC pathway being the most common (Yin et al., 2022). In this sense, the MMC pathway transforms propionate into acetate and hydrogen, rather than through C6 dismutation, where butyrate can be degraded into acetate and hydrogen (Jin and Lu, 2023).

The low microorganism proportion, such as the *Chloroflexi* phylum, is closely involved in polysaccharides and monosaccharides decomposition as well as the production of acetic acid. Although several types of research describe *Chloroflexi* as one of the main phyla in anaerobic reactors, its metabolic functions have been barely described. The most common *Chloroflexi* relative abundance reported is in the range of 20–25 % (Zheng et al., 2015; Wang et al., 2018; Chen et al., 2020), being involved in lignocellulosic degradation studies. Our results showed a low proportion of *Chloroflexi* microorganisms during the experiment, with percentages of 8 %, 6 %, 4 %, 3 %, 2 %, and 2 % related to the nZVI, F_3O_4-NP, nZVI/F_3O_4-NP, control, blank, and inoculum samples, respectively. Despite its low proportion, nZVI treatment showed significant differences between the control and blank samples, demonstrating the effect of Fe-NPs on the sludge. According to Jackson et al. (2020), *Spirochaetes* are stimulated by acetic acid production, suggesting a possible acetate oxidation process. These microorganisms have rarely been studied due to the limited understanding of the anaerobic fermentation process and the scarcity of reports. Nonetheless, they are assumed to be glucose fermenters based on findings in response to the glucose addition (Lee et al., 2013). Since the presence of acetate significantly increases in the nZVI digestors (4 %), it causes an increased abundance of acetate-oxidizing spirochaetes in these systems compared to the control (1 %). These consequences further explain why Fe-NPs are the most prominent additives used to boost the performance of anaerobic fermentation. This insight can encourage the presence of specific microorganisms and inhibit others, thereby modifying the production of VFAs.

4.3. Potential mechanisms underlying microbial and metabolic shifts induced by Fe-NP addition

Our observations of propionate degradation accompanied by acetate accumulation in the absence of active methanogens are consistent with the literature, which describes enhanced syntrophic metabolism mediated by CMs (Guo et al., 2021; Wang et al., 2023). Previous studies have demonstrated that *Syntrophomonas* and members of the *Desulfobacterota* possess genetic and physiological traits that enable extracellular electron transfer, and that Fe-based nanoparticles stimulate their activity during fatty acid oxidation (Guo et al., 2021; Akram et al., 2024). Although DIET between fermentative partners has not yet been unequivocally demonstrated, our results strongly suggest that Fe-NPs facilitated an alternative electron transfer route beyond classical IHT/IFT. This interpretation aligns with the proposed role of DIET-like mechanisms in accelerating propionate oxidation and redirecting carbon flow toward acetate, even when methanogenesis is absent.

The proliferation of microorganisms such as *Syntrophobacter, Desulfobacterota,* and *Hydrogenisphora* could occur due to the stimulatory effect observed under Fe-NPs supplementation, which can therefore be attributed to alternative mechanisms. First, Fe^{3+}/Fe^{2+} cycling derived from nanoparticle dissolution likely acted as an abiotic electron sink, enabling fermentative bacteria to maintain redox balance without relying on DIET (Gahlot et al., 2020). Second, classical IHT/IFT remains a plausible route for electron disposal, as fermentative microorganisms typically release these intermediates during the production of VFAs (Akram et al., 2024). The presence of Fe-NPs can abiotically consume or transform hydrogen, preventing feedback inhibition and supporting continued fermentation. Notably, nZVI readily forms iron (hydro)oxide on its surface due to oxidation, thereby accelerating hydrogen release (Chen et al., 2020; Hoffmann et al., 2022).

The microbial community data further support this interpretation. The increase in *Syntrophobacter* relative abundance under nZVI treatment suggests stimulation of syntrophic propionate-oxidizing bacteria, which depend on efficient H_2 and formate removal to

Table 1
VFAs production via anaerobic fermentation amended with Fe-NPs.

Time	Treatment	Acetic acid	Propionic acid	Butyric acid	Iso-Valeric acid	Valeric acid	Total VFA	AE
[days]		COD [mg COD L^{-1}]	COD [mg COD L^{-1}]	COD [mg COD L^{-1}]	COD [mg COD L^{-1}]	COD [mg COD L^{-1}]	COD [mg COD L^{-1}]	[%]
4	nZVI	196.8 ± 47.3 Aa	63.9 ± 11.9 ABab	31.0 ± 0.0 Cb	42.2 ± 4.4 Ab	0.0 ± 0.0 Aa	321.9 ± 61.42 Aa	21,29 % ± 4,06 %
	Fe_3O_4	195.5 ± 46.77 Aa	36.1 ± 20.4 Aab	0.0 ± 0.0 Aa	0.0 ± 0.0 Aa	0.0 ± 0.0 Aa	231.6 ± 60.0 Aa	15,32 % ± 3,97 %
	nZVI/Fe_3O_4	165.3 ± 51.3 ABa	56.9 ± 6.1 ABb	0.0 ± 0.0 Aa	35.1 ± 4.3 Ab	0.0 ± 0.0 Aa	257.5 ± 60.6 Aa	17,03 % ± 4,01
	Control	119.7 ± 2,3 Aa	31.6 ± 6.7 Aa	0.0 ± 0.0 Aa	36.7 ± 4.7 Ab	0.0 ± 0.0 Aa	188.0 ± 9.8 Aa	12,43 ± 0,65
	Blank	166.8 ± 51.5 ABa	62.4 ± 8.9 Ab	0.0 ± 0.0 Aa	35.6 ± 4.3 Ab	0.0 ± 0.0 Aa	264.8 ± 61.3 Aa	17,51 % ± 4,08
6	nZVI	214.4 ± 42.1 Aa	60.7 ± 7.5 Aa	0.0 ± 0.0 Ba	46.0 ± 4.7 Ab	0.0 ± 0.0 Aa	321.1 ± 49.5 Aa	21,24 % ± 3,27 %
	Fe_3O_4	227.9 ± 47.5 Aa	56.1 ± 15.2 Aa	0.0 ± 0.0 Aa	0.0 ± 0.0 Aa	0.0 ± 0.0 Aa	284.0 ± 62.7 ABa	18,78 % ± 4,14 %
	nZVI/Fe_3O_4	279.6 ± 80.1 ABa	89.7 ± 25.7 ACa	33.4 ± 6.6 Bb	50.3 ± 9.4 Ab	0.0 ± 0.0 Aa	453.6 ± 121.9 Aa	29,96 % ± 8,06 %
	Control	302.4 ± 39.9 Ba	61.3 ± 13.0 Aa	28.4 ± 3.6 Bb	49.9 ± 24.7 Ab	0.0 ± 0.0 Aa	442.0 ± 61.1 Aa	29,23 % ± 4,04 %
	Blank-	202.5 ± 27.5 Ba	76.2 ± 10.3 ABa	16.5 ± 14.3 Aa	0.0 ± 0.0 Ba	0.0 ± 0.0 Aa	295.2 ± 21.1 ABa	19,53 % ± 1,33 %
12	nZVI	**262.2 ± 96.5 Aa**	**59.3 ± 16.8 Aab**	30.5 ± 9.6 ABCa	0.0 ± 0.0 Ba	0.0 ± 0.0 Aa	352.1 ± 100.3 Aa	23,29 % ± 6,63 %
	Fe_3O_4	**295.5 ± 12.7 Aa**	**119.1 ± 68.3 ABab**	0.0 ± 0.0 Aa	61.6 ± 26.2 Aab	0.0 ± 0.0 Aa	476.2 ± 104.1 ABa	31,50 % ± 6,88 %
	nZVI/Fe_3O_4	250.2 ± 18.7 Ba	97.6 ± 15.1 CDab	34.1 ± 0.9 Bb	104.8 ± 63.7 Aab	0.0 ± 0.0 Aa	486.2 ± 77.2 Aa	32,19 % ± 5,11 %
	Control	233.1 ± 73.8 ABa	61.8 ± 2.6 Ba	0.0 ± 0.0 Aa	56.7 ± 10.4 Ab	0.0 ± 0.0 Aa	351.6 ± 100.3 Aa	23,25 % ± 5,40 %
	Blank	252.8 ± 28.5 Ba	105.1 ± 4.0 Bb	0.0 ± 0.0 Aa	0.0 ± 0.0 Ba	0.0 ± 0.0 Aa	357.9 ± 30.1 Aa	23,67 % ± 1,99 %
25	nZVI	**253.7 ± 47.2 Ab**	**302.6 ± 19.7 Bb**	35.5 ± 1.6 Ab	**124.1 ± 63.7 ABa**	50.4 ± 21.1 Aab	**769.9 ± 41.3 Ba**	**50,92 % ± 2,73 %**
	Fe_3O_4	**349.8 ± 22.5 Ab**	**244.3 ± 9.3 Bb**	33.7 ± 6.2 Bb	**121.1 ± 47.7 Aa**	62.9 ± 13.6 Bb	**811.7 ± 99.2 Bab**	**53,69 ± 6,56 %**
	nZVI/Fe_3O_4	82.73 ± 23.4 Ab	76.1 ± 25.6 BDa	36.7 ± 5.1 Bb	**39.3 ± 8.7 Ab**	0.0 ± 0.0 Aa	**455.7 ± 44.1 Abc**	**30,14 % ± 2,91 %**
	Control	216.1 ± 27.04 ABab	183.2 ± 31.6 Aab	35.2 ± 7.8 Bb	74.6 ± 47.6 Aa	41.7 ± 18.4 Bab	**550.8 ± 84.3 Aab**	**27,60 % ± 14,98 %**
	Blank	0.0 ± 0.0 Aa	106.9 ± 11.0 Ba	0.0 ± 0.0 Aa	0.0 ± 0.0 Ba	0.0 ± 0.0 Aa	**106.9 ± 11.0 Cc**	**7,07 % ± 0,72 %**

Different letters imply significant differences.
Uppercase letters indicate differences between treatment times
Lowercase letters indicate differences between treatments

sustain metabolism (Chen et al., 2022). Similarly, the presence of *Hydrogenispora*, a genus associated with acetogenic production, indicates that carbohydrate and ethanol fermentation to acetate was favored under Fe-NP amendment (Li et al., 2020). These findings reinforce the notion that Fe-NPs indirectly enhanced the activity of fermentative and syntrophic bacteria by stabilizing electron disposal routes. Additionally, Fe is a crucial cofactor for key fermentative enzymes, such as hydrogenases and dehydrogenases, and its increased availability from Fe-NP dissolution may enhance enzymatic activity and overall metabolic rates (Chen et al., 2022). Taken together, these results suggest that under methanogenesis-inhibited conditions, Fe-NPs stimulate fermentative metabolism primarily through redox buffering, IHT/IFT stabilization, and micronutrient supply, which in turn explains both the microbial community shifts (e.g., enrichment of *Syntrophobacter* and *Hydrogenispora*) and the enhanced VFAs accumulation observed in our experiments.

The combined nZVI/Fe_3O_4 treatment did not enhance VFAs accumulation compared to single nanoparticle supplementation. A possible explanation lies in the imbalance of intracellular redox potential (NAD^+/NADH) caused by the simultaneous presence of both electron-donating (nZVI) and electron-shuttling (Fe_3O_4) materials (Tejedor-Sanz et al., 2022). Excessive electron availability from nZVI dissolution, together with rapid electron transfer via Fe_3O_4, may have disrupted the optimal NAD^+/NADH balance required for stable fermentation pathways (Cao et al., 2025). This imbalance could limit the efficiency of oxidation routes and redirect metabolic activity away from VFAs production. Although NAD^+/NADH levels were not measured in this study, future experiments should incorporate redox cofactor monitoring to understand better how nanoparticle combinations affect intracellular metabolism and to clarify the mechanistic basis of the reduced performance observed with the nZVI/Fe_3O_4 mixture.

5. Conclusions

This study investigated the impact of nZVI, Fe_3O_4-NPs, and nZVI/Fe_3O_4-NPs single doses on VFAs production via AF. Our results demonstrate that the amendment of nZVI and Fe_3O_4-NPs can also strategically redirect anaerobic fermentation toward the production of valuable VFAs. In this sense, nZVI treatment showed an effective increase in acetic acid production and Fe_3O_4-NP in propionic acid production, whereas nZVI/Fe_3O_4-NPs treatment showed no effect on VFA production. Moreover, the iron nanoparticles effectively alter the microbial communities during anaerobic fermentation, enhancing the diversification of the population.

Funding resources

This work was supported by ANID/FONDAP/1523A0001, the Chilean Association of Science and Development (ANID) under the scope of ANID Fondecyt Regular 1231521, the National Doctoral Scholarship ANID21202184, the ANID/FONDAP/15130015, Fondecyt Postdoctoral project 3230478, and ATE220038. The project from the University of La Frontera, PP24–0007, and ANID/FOVI220003. This research was also supported by the Portuguese Foundation of Science and Technology (FCT) under the scope of the CM4Methane project (Ref: PTDC/BTA-BTA/2249/2021, DOI: https://doi.org/10.54499/PTDC/BTA-BTA/2249/2021.

CRediT authorship contribution statement

Gustavo Ciudad: Writing – review & editing, Supervision, Resources, Methodology, Funding acquisition, Conceptualization. **Rodrigo Rodriguez:** Methodology, Formal analysis. **Paola Durán:** Resources, Methodology, Formal analysis, Conceptualization. **Braga Catia Sofia Neves:** Writing – review & editing, Supervision. **Gilberto Martins:** Writing – review & editing, Supervision, Methodology, Conceptualization. **Lina Uribe:** Formal analysis, Software, Writing – review & editing. **Olga Rubilar:** Writing – review & editing, Supervision, Resources, Methodology, Investigation, Funding acquisition. **Hoffmann Nicolas:** Writing – original draft, Validation, Methodology, Investigation, Formal analysis, Data curation, Conceptualization. **Christian Vergara:** Writing – review & editing, Methodology, Conceptualization. **Paola Fincheira:** Writing – review & editing, Supervision, Formal analysis. **Gonzalo Tortella:** Writing – review & editing, Supervision.

Declaration of Competing Interest

The authors declare that they have no known competing financial interests or personal relationships that could have appeared to influence the work reported in this paper.

Acknowledgments

None

Data availability

No data was used for the research described in the article.

References

Akram, J., Song, C., El Mashad, H.M., Chen, C., Zhang, R., Liu, G., 2024. Advances in microbial community, mechanisms and stimulation effects of direct interspecies electron transfer in anaerobic digestion. Biotechnol. Adv. 76, 108398. https://doi.org/10.1016/j.biotechadv.2024.108398.

Alam, M., Dhar, B.P., 2023. Boosting thermophilic anaerobic digestion with conductive materials: current outlook and future prospects. Chemosphere 343, 140175. https://doi.org/10.1016/j.chemosphere.2023.140175.
Barrena, R., Vargas-García, M.C., Capell, G., Baranska, M., Puntes, V., Moral-Vico, J., Sánchez, A., Font, X., 2021. Sustained effect of zero-valent iron nanoparticles under semi-continuous anaerobic digestion of sewage sludge: evolution of nanoparticles and microbial community dynamics. Sci. Total Env. 777, 145969. https://doi.org/10.1016/j.scitotenv.2021.145969.
Bolyen, E., Rideout, J., Dillon, M., Bokulich, N., Abnet, C., Al-Ghalith, G., Alexander, H., Alm, E., Arumugam, M., Asnicar, F., et al., 2019. Reproducible, interactive, scalable and extensible microbiome data science using QIIME 2. Nat. Biotechnol. 37, 852–857. https://doi.org/10.1038/s41587-019-0209-9.
Braga, C., Martins, G., Soares, S., Pereira, F., Pereira, I., Pereira, L., Alves, M., Salvador, A., 2024. Non-conductive silicon-containing materials improve methane production by pure cultures of methanogens. Bioresour. Technol. 408, 131144. https://doi.org/10.1016/j.biortech.2024.131144.
Cao, J., Zhang, C., Li, X., Dai, X., Xu, Y., 2025. Microbial community and metabolic pathways in anaerobic digestion of organic solid wastes: progress, challenges, and prospects. Fermentation 11 (8), 457. https://doi.org/10.3390/fermentation11080457.
Chen, L., Fang, W., Chang, J., Liang, J., Zhang, P., Zhang, G., 2022. Improvement of direct interspecies electron transfer via adding conductive materials in anaerobic digestion: mechanisms, performances, and challenges. Front. Microbiol 13, 860749. https://doi.org/10.3389/fmicb.2022.860749.
Chen, Y., Yang, Z., Zhang, Y., Xiang, Y., Xu, R., Jia, M., Cao, J., Xiong, W., 2020. Effects of different conductive nanomaterials on anaerobic digestion process and microbial community of sludge. Bioresour. Technol. 304, 123016. https://doi.org/10.1016/j.biortech.2020.123016.
Du, X., Zhang, Y., Ma, Y.-W., Feng, S.-X., Zhang, Y.-X., Kou, H.-J., Sun, Y., 2023. The synergistic effect of chemical oxidation and microbial activity on improving volatile fatty acids (VFAs) production during the animal wastewater anaerobic digestion process treated with persulfate/biochar. Sci. Total Environ. 857, 159276. https://doi.org/10.1016/j.scitotenv.2022.159276.
Edgar, R.C., 2016. UNOISE2: Improved error-correction for Illumina 16S and ITS amplicon sequencing. bioRxiv. https://doi.org/10.1101/081257.
Eljamal, O., Eljamal, R., Falyouna, O., Maamoun, I., Thompson, I.P., 2024. Exceptional contribution of iron nanoparticle and Aloe vera biomass additives to biogas production from anaerobic digestion of waste sludge. Energy 30, 131761. https://doi.org/10.1016/j.energy.2024.131761.
Esteban-Gutierrez, M., Garcia-Aguirre, J., Irizar, I., Aymerich, E., 2018. From sewage sludge and agri-food waste to VFA: individual acid production potential and up-scaling. Waste Manag 77, 203–212. https://doi.org/10.1016/j.wasman.2018.05.027.
Feng, S., Ngo, H.H., Guo, W., Chang, S.W., Nguyen, D.D., Liu, Y., Zhang, S., Vo, H.N.P., Bui, X.T., Hoang, B.N., 2022. Volatile fatty acids production from waste streams by anaerobic digestion: a critical review of the roles and applications of enzymes. Bioresour. Technol. 359, 127420. https://doi.org/10.1016/j.biortech.2022.127420.
Gahlot, P., Ahmed, B., Tiwari, S.B., Aryal, N., Khursheed, A., Kazmi, A.A., Tyagi, V.K., 2020. Conductive material engineered direct interspecies electron transfer (DIET) in anaerobic digestion: mechanism and application. Env. Technol. Innov. 20, 101056. https://doi.org/10.1016/j.eti.2020.101056.
García, A., Ruíz, C., Hermosilla, D., Muñoz, R., de Godos, I., 2023. Simultáneous production of biogas and volatile fatty acids through anaerobic digestion using cereal straw as substrate. Env. Techn. Innov. 31, 103215. https://doi.org/10.1016/j.eti.2023.103215.
Guo, X., Chen, H., Zhu, X., Xia, A., Liao, Q., Huang, Y., Zhu, X., 2021. Revealing the role of conductive materials on facilitating direct interspecies electron transfer in syntrophic methanogenesis: a thermodynamic analysis. Energy 229, 120747. https://doi.org/10.1016/j.energy.2021.120747.
Hoffmann, N., Braga, S.N., Rubilar, O., Ciudad, G., Tortella, G., Hermosilla, E., Duarte, M.S., Pereira, L., Salvador, A.F., Martins, G., 2025. Challenging the conductive paradigm; the unexpected role of sand in anaerobic digestion. Bioresour. Technol. 438, 133163. https://doi.org/10.1016/j.biortech.2025.133163.
Hoffmann, N., Fincheira, P., Tortella, G., Rubilar, O., 2022. The role of iron nanoparticles on anaerobic digestion: mechanisms, limitations, and perspectives. Env. Sci. Pollut. Res. 29, 82619–82631. https://doi.org/10.1007/s11356-022-23302-3.
Jackson, S.A., Kang, X., O'Shea, R., O'Leary, N., Murphy, J.D., Dobson, A., D.W, 2020. Anaerobic digestion performance and microbial community structures in biogas production from whiskey distillers organic by-products. Bioresour. Technol. Rep. 12, 100565. https://doi.org/10.1016/j.biteb.2020.100565.
Jin, B., Jia, Y., Cheng, K., Chu, C., Wang, J., Liu, Y., Du, J., Wang, L., Pang, L., Ji, J., Cao, X., 2024. Facilitating synergy effects with zero-valent iron and peroxysulfate on the sludge anaerobic fermentation system: combined biological enzyme, microbial community and fermentation mechanism assessment. Chemosphere 355, 141805. https://doi.org/10.1016/j.chemosphere.2024.141805.
Jin, Y., Lu, Y., 2023. Syntrophic propionate oxidation: one of the rate-limiting steps of organic matter decomposition in anoxic environments. Appl. Environ. Microbiol 89, e0038423. https://doi.org/10.1128/aem.00384-23.
Kang, Y.-R., Su, Y., Wang, J., Chu, Y.-X., Tian, G., He, R., 2021. Effects of different pretreatment methods on biogas production and microbial community in anaerobic digestion of wheat straw. Env. Sci. Pollut. Res. 23, 51772–51785. https://doi.org/10.1007/s11356-021-14296-5.
Katoh, K., Standley, D., 2013. MAFFT multiple sequence alignment software version 7: Improvements in performance and usability. Mol. Biol. Evol. 30, 772–780. https://doi.org/10.1093/molbev/mst010.
Kim, J., Rhee, S.K., Lee, H.J., Lee, S.Y., Lee, Y., 2022. Syntrophic propionate oxidation: a review. Front. Microbiol. 13, 968416. https://doi.org/10.3389/fmicb.2022.968416.
Lee, S.-H., Park, J.-H., Kang, H.-J., Lee, Y.H., Lee, T.J., Park, H.-D., 2013. Distribution and abundance of spirochaetes in full-scale anaerobic digesters. Bioresour. Technol. 145, 25–32. https://doi.org/10.1016/j.biortech.2013.02.070.
Li, Y., Zhu, Q., Ding, P., You, S., Zhang, Q., Jiang, H., 2020. Effects of Fe^0 and Ni^0 nanoparticles on hydrogen production from cotton stalk hydrolysate using *Klebsiella sp*. WL1316: evaluation of size and concentration of the nanoparticles. Int. J. Hydrog. Energy 45 (11), 6243–6253. https://doi.org/10.1016/j.ijhydene.2020.01.012.
Oksanen, J., Simpson, G.L., Blanchet, F.G., Kindt, R., Legendre, P., Minchin, P.R., O'Hara, R.B., Solymos, P., Stevens, M.H.H., Szoecs, E., Wagner, H., Barbour, M., Bedward, M., Bolker, B., Borcard, D., Carvalho, G., Chirico, M., De Caceres, M., Durand, S., Evangelista, H.B.A., FitzJohn, R., Friendly, M., Furneaux, B., Hannigan, G., Hill, M.O., Lahti, L., McGlinn, D., Ouellette, M.-H., Ribeiro Cunha, E., Smith, T., Stier, A., Ter Braak, C.J.F., Weedon, J., 2022. Vegan: Community ecology package (R package version 2.6-4). ⟨https://CRAN.R-project.org/package=vegan⟩.
Omondi, E.A., Ndiba, P.K., Gikuma-Njuru, P., Abuga, D., 2020. Dynamics of microbial communities in co-digestion of water hyacinth (Eichhornia crassipes) with rumial slaughterhouse waste under mesophilic conditions. Int. J. Water Res. Env. Eng. 12, 81–89. https://doi.org/10.5897/IJWREE2020.0946.
Paulson, J., Stine, O., Bravo, H., Pop, M., 2013. Robust methods for differential abundance analysis in marker gene surveys. Nat. Methods 10, 1200–1202. https://doi.org/10.1038/nmeth.2658.
Pinto, A.S., McDonald, L.J., Jones, R.Y., Massanet-Nicolau, J., Guwy, A., McManus, M., 2023. Production of volatile fatty acids by anaerobic digestion of biowastes: Techno-economic and life cycle assessment. Bioresour. Technol. 388, 129726. https://doi.org/10.1016/j.biortech.2023.129726.
Price, M., Dehal, P., Arkin, A., 2009. FastTree: computing large minimum evolution trees with profiles instead of a distance matrix. Mol. Biol. Evol. 26, 1641–1650. https://doi.org/10.1093/molbev/msp077.
Pruesse, E., Quast, C., Knittel, K., Fuchs, B., Ludwig, W., Peplies, J., Glöckner, F., 2007. SILVA: A comprehensive online resource for quality checked and aligned ribosomal RNA sequence data compatible with ARB. Nucleic Acids Res. 35, 7188–7196. https://doi.org/10.1093/nar/gkm864.
Segata, N., Izard, J., Waldron, L., Gevers, D., Miropolsky, L., Garrett, W., Huttenhower, C., 2011. Metagenomic biomarker discovery and explanation. Genome Biol. 12, R60. https://doi.org/10.1186/gb-2011-12-6-r60.
Tejedor-Sanz, S., Stevens, E.T., Li, S., Finnegan, P., Nelson, J., Knoesen, A., Light, S.H., Ajo-Franklin, C.M., Marco, M.L., 2022. Extracellular electron transfer increases fermentation in lactic acid bacteria via a hybrid metabolism. eLife 11, e70684. https://doi.org/10.7554/eLife.70684.
Valentino, F., Munarin, G., Marco, B., Cavinato, C., Bolzonella, D., Pavan, P., 2021. Enhancing volatile fatty acids (VFAs) production from food waste in a two-phase pilot-scale anaerobic digestion process. J. Env. Chem. Eng. 9, 106062. https://doi.org/10.1016/j.jece.2021.106062.
Wang, P., Li, X., Su, Y., Wu, D., Xie, B., 2023. Enhanced anaerobic digestion performance of food waste by zero-valent iron and iron oxides nanoparticles: Comparative analyses of microbial community and metabolism. Bioresour. Technol. 371, 128633. https://doi.org/10.1016/j.biortech.2023.128633.
Wang, P., Yu, Z., Zhao, J., Zhang, H., 2018. Do microbial communities in an anaerobic bioreactor change with continuous feeding sludge into full-scale anaerobic digestion system? Bioresour. Technol. 249, 89–98. https://doi.org/10.1016/j.biortech.2017.09.191.

Wang, R., Li, Ch, Lv, N., Pan, X., Cai, G., Ning, J., Zhu, G., 2021. Deeper insights into the effect of activated carbon and nano-zero valent iron addition on acidogenesis and whole anaerobic digestion. Bioresour. Technol. 324, 124671. https://doi.org/10.1016/j.biortech.2021.124671.

Wiegel, J., Tanner, R., Raine, F.A., 2006. An introduction to the family clostridiaceae. In: Book: Prokaryotes, 4. Springer, pp. 654–678. https://doi.org/10.1007/0-387-30744-3_20.

Yin, J., Li, J., Qiu, X., Zhou, Y., Wang, M., Feng, H., Li, Y., Chen, X., Chen, T., 2022. Effect of magnetite particle size on propionate degradation in the propionate-based anaerobic system. Sci. Total Env. 847, 157592. https://doi.org/10.1016/j.scitotenv.2022.157592.

Zheng, Z., Liu, J., Yuan, X., Wang, X., Zhu, W., Yang, F., Cui, Z., 2015. Effect of dairy manure to switchgrass co-digestion ratio on methane production and the bacterial community in the batch anaerobic digestion. Appl. Energy 151, 249–257. https://doi.org/10.1016/j.apenergy.2015.04.078.

Zhou, X., Guo, M., Fu, X., Wang, D., Liao, J., Xu, W., Han, H., 2024. Insights into microbial metabolic coordination under driving force of different conductive materials-mediated direct interspecies electron transfer during anaerobic digestion. Chem. Eng. J. 496, 154230. https://doi.org/10.1016/j.cej.2024.154230.

Zhu, X., Blanco, E., Bhatti, M., Borrion, A., 2021. Impact of metallic nanoparticles on anaerobic digestion: a systematic review. Sci. Total Env 757, 143747. https://doi.org/10.1016/j.scitotenv.2020.143747.